The Development of Texture in Co–Cr Films

Li Cheng-Zhang, J. C. Lodder, and J. A. Szpunar

Abstract—**Texture development as a function of film thickness (5–980 nm) was investigated for two series of $Co_{81}Cr_{19}$ films. In general, the films were strongly textured. The orientation ratio, OR_c, was used to describe the strength of the texture. Experimental data showed that for the Series A films (5–200 nm), the OR_c value increased with increasing film thickness, while for Series B films (46–980 nm), the OR_c as a function of the film thickness described a single peak curve, with its maximum near 130 nm. The calculated local orientation ratios OR_{cx} for both the Series A and B films had maxima near 110 nm. The strain in Co–Cr films also changes with the film thickness. In the case of the Series B films, the strain along the film normal gradually changed from a tensile to a compressive strain with increasing film thickness, and near 130 nm the film was in a stress-free condition. It was also discovered that for Co–Cr films thinner than 46 nm, the aspect ratio of the grains approaches 1 and the typical columnar structure of grains is not observed, although (0002) fibre texture still exists.**

Introduction

IT is important to understand the nucleation mechanism and the process of grain growth in thin films as the developed microstructure will control the resulting magnetic properties. At present, the magnetic thin films used in both longitudinal and perpendicular recording media are polycrystalline and have a thickness in the range of 15–240 nm [1], [2], and recent increases in the recording density of magnetic disks pushes this range to even thinner films. The magnetic and mechanical properties of these thin films can vary, depending on the condition of the film-deposition process, the composition, the microstructure, the grain morphology and the texture.

Previous investigations [6], [9]–[12] have demonstrated that Co–Cr films display a columnar microstructure with a strong degree of alignment of the C-axis in the direction perpendicular to the film normal. The high degree of texture in Co–Cr films plays a major role in optimizing their magnetic properties.

There is clear experimental evidence [5]–[7] that Co–Cr film texture is closely related to the choice of the substrate and/or seedlayer. In general, the dispersion of the orientation of the hcp C-axis formed by the "layer-island" growth mechanism is smaller than that for the "island" growth mechanism. It has been shown [6] that for specimens with a Co–Cr/Si structure, the growth of the columnar grains can be described by the "layer-island" growth mechanism.

Texture develops as a result of competition between nuclei and grains having different orientation. In order to describe the growth mechanism, the textural evolution and changes in strain were studied for five Series of Co–Cr films. Our research concentrated on the investigation of the following:

a) The textural changes as a function of the film thickness for Co–Cr films having the same average composition.
b) The textural changes in films having different compositions, but having the same thickness.
c) The influence of the substrate and/or seedlayer on the texture of Co–Cr films with the same thickness.
d) The influence of different preparation methods (i.e., both sputtering and two-beam obliquely co-evaporation methods) on the textural evolution.
e) The correlation between textural development, strain distribution and magnetic properties in Co–Cr films.

In this report, we describe the textural evolution with the thickness for $Co_{81}Cr_{19}$ films. Research on other topics will be reported in other papers [10], [12].

Experimental Procedure

Two series of $Co_{81}Cr_{19}$ films, obtained by sputtering, were chosen to investigate textural evolution and the change in strain with film thickness. The average nominal composition for all tested specimens was $Co_{81}Cr_{19}$. The preparation conditions were as follows: P_{ar} (Argon pressure) = 4×10^{-3} mbar, voltage, V_{rf} = 1.6 kV and T_s (substrate temperature) = 150°C. The Series A and B films were deposited on $Ge/SiO_2/Si$ and Si substrates. The thickness of the films and the surface roughness were measured using STM (scanning tunneling microscope) and AFM (atomic force microscope) methods. The thicknesses for Series A and B are in the range of 5–200 nm and 46–980 nm, respectively. The maximum surface roughness for the thinnest films is about 6 nm and increases with increasing film thickness up to about 50 nm. The magnetic properties were measured by a VSM and a torque magnetometer. The maximum applied field was about 840 kA/m. The coercivities H_c for all tested films

Manuscript received August 19, 1992; revised September 21, 1993.

L. Cheng Zeng is on leave from Institute of Computing Technology, Academia Sinica, P.O. Box 2704-6, Beijing, P.R. China 100080. He is currently with Department Metallurgical Eng., McGill University, 3450 University Street, Montreal, PQ, Canada, H3A 2A7.

J. C. Lodder is with MESA Research Institute, Faculty of Electrical Eng., University of Twente, P.O. Box 217, 7500 AE Enschede, The Netherlands.

J. A. Szpunar is with Department Metallurgical Eng., McGill University, 3450 University Street, Montreal, PQ, Canada, H3A 2A7.

IEEE Log Number 9400798.

TABLE I
PROPERTIES FOR SERIES A $Co_{81}Cr_{19}$ FILMS

No	Thickness (nm)	M_s kA/m	$H_{c\perp}$ kA/m	$H_{c\parallel}$ kA/m	K_1 kJ/m^3	$R_{s\perp}$
A_1	5	360	4.0	3.1	122	1.0
A_2	12	460	4.3	1.7	116	0.02
A_3	25	500	15.4	16.8	127	0.06
A_4	50	480	36.8	12.9	110	0.11
A_5	100	510	47.2	11.8	134	0.12
A_6	200	500	69.9	12	131	0.17

TABLE II
PROPERTIES FOR SERIES B $Co_{81}Cr_{19}$ FILMS

No	Thickness (nm)	M_s kA/m	$H_{c\perp}$ kA/m	$H_{c\perp}$ kA/m	K_1 kJ/m^3	$R_{s\perp}$
B_1	46	450	79	7	94	0.26
B_2	110	470	96	6	115	0.25
B_3	300	445	65	6	99	0.16
B_4	610	435	46	7	84	0.11
B_5	980	430	40	7	86	0.10

range from 4 to 96 kA/m. The most relevant properties of the two Series of $Co_{81}Cr_{19}$ films are presented in Tables 1 and 2. $R_{s\perp}$ is the squareness ratio ($M_{r\perp}/M_s$) in the direction normal to the film plane. $H_{c\perp}$ and $H_{c\parallel}$ are the coercivities in the direction normal to the film and the in-plane direction, respectively.

To investigate the crystallographic texture, all specimens were first measured using a Rigaku diffractomer (Cu–K_α radiation) to determine the crystalline structure. The (0002) pole figure of the same specimens were then measured using a Siemens D-500 texture goniometer (*Mo–*K_α radiation). The measured pole figures show a strong maxima in the central part, and this range was then remeasured over 12° angular intervals as a function of the specimen tilt angle α (i.e., the radial angle of the pole figure). The ratio OR_c (α, β) of the pole density $F(\alpha, \beta)$ of the film to the pole density of a random specimen was used to evaluate the orientation ratio using the following expression:

$$OR_c(\alpha, \beta) = \frac{\left(\frac{1}{\alpha_1 - \alpha_2}\right) \int_{\alpha_1}^{\alpha_1} \int_0^{2\pi} F(\alpha, \beta)\, d\alpha\, d\beta}{\frac{2}{\pi} \int_0^{\pi/2} \int_0^{2\pi} F(\alpha, \beta)\, d\alpha\, d\beta}, \quad (1)$$

where β is the circumferential angle of the pole figure. In our case, the value of $F(\alpha, \beta)$ is assumed to be equal to the value of $F(\alpha)$, since the texture in the α-Co phase exhibits high degree of rotational symmetry around the film normal. For the sake of convenience, the maximum of the $OR_c(\alpha, \beta)$ value defined in (1) will be called the orientation ratio OR_c of the crystallites for the (0002) plane.

RESULTS AND DISCUSSION

The measured relation between the columnar diameter and thickness for Series B films is illustrated in Fig. 1.

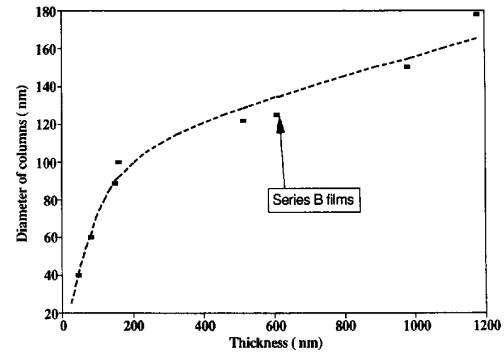

Fig. 1. The dependence of the columnar diameter on the thickness for Series B $Co_{81}Cr_{19}$ films.

As expected, the diameter of the columnar grain increases with increasing film thickness in the range of 46–980 nm, but the rate of increase of this diameter for films thinner than 200 nm is much higher than that in films thicker than this. Thus during the initial stages of grain growth, the grains grow fastest in the direction parallel to the film surface but this growth rate gradually decreases and approaches a saturation value for film thicknesses greater than 500 nm. Similar results were also reported in reference [15].

Two columnar growth mechanisms have been observed. In the first case cross-sectional TEM and SEM-micrographs showed [6], [11] that the columns in sputtered Co–Cr films stretch straight upwards and have a near constant diameter along the columnar length. Other SEM investigations [15] have shown that the columns increase slightly in diameter towards the film surface from bottom to top. The grains in our specimens belonged to this category of conically shaped columns. Since the columnar grains were observed growing throughout the thickness of all specimens it is reasonable to assume that the length of a column in a Co–Cr film is equal to the film thickness. Based on this assumption the ratio T/D of the grain length T to diameter D, the "aspect ratio," was calculated. As shown in Fig. 2, the aspect ratio as a function of the film thickness for the Series B films exhibited a linear relationship for films up to about 1000 nm. As the thickness decreased to 40 nm, the aspect ratio approaches 1 and the grains tend to form an equiaxed crystallite structure.

Diffraction spectra were used to identify crystallographic phases in the films. Typical diffraction spectra for specimens A_5 (100 nm) and A_1 (5 nm) are shown in Figs. 3 and 4(a), respectively. To distinguish between the diffraction spectra of the Co–Cr film and the Si substrate, the diffraction spectrum for the Si substrate is shown in Fig. 4(b). It can be observed from these diffraction patterns that the (0002) and (0004) maxima for hcp α-Co structures are identified. The (200) and (400) maxima of the cubic structure of the Si substrate can also be identified. Furthermore, the FCC diffraction maxima for the CoO phase can be identified by the presence of (220) planes.

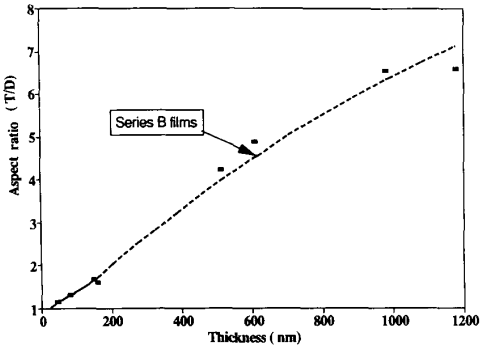

Fig. 2. The dependence of the aspect ratio on the thickness for Series B $Co_{81}Cr_{19}$ films.

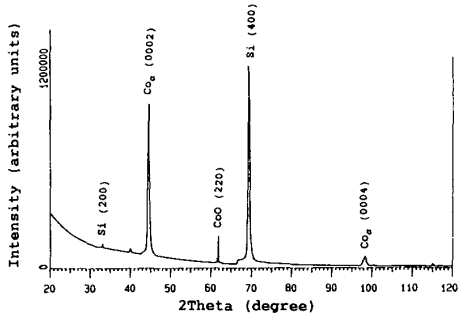

Fig. 3. The diffraction spectrum for specimen A_5 (100 nm).

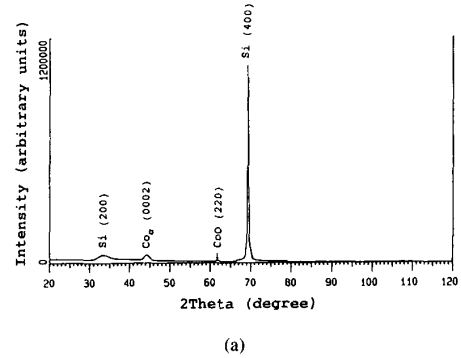

(a)

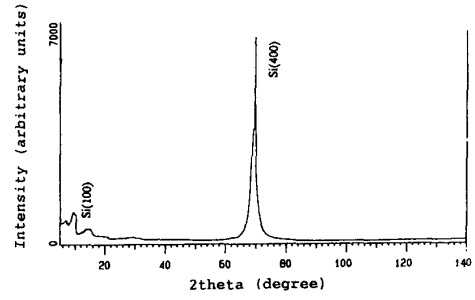

(b)

Fig. 4. (a) The diffraction spectrum for specimen A_1 (5 nm). (b) The diffraction spectrum for Si substrates.

Varying the film thickness shifts the peak (0002). For both series a systematic increase in the (0002) peak position is observed with increasing film thickness, as is shown by experimental data in Tables III and IV.

Two possible effects could influence this (0002) peak position shift. The first [14] is the existence of an FCC Co phase in the $Co_{81}Cr_{19}$ films. In our case, however, the measured diffraction spectra can not furnish any evidence to support this case. The other explanation for the peak shift is the existence of internal stresses within the films. When a Co-Cr film is subjected to a tensile or compressive stress, the lattice plane spacing in the grains will change from their stress-free value to a new value corresponding to the magnitude and sign of the applied stress. This macrostrain leads to a shift of the diffraction lines to new 2θ positions. Internal stress in a Co-Cr film is usually closely related to the type of the substrate and/or the seedlayer.

Based on the peak-shift data listed in Tables III and IV, and diffraction pattern of annealed powders, the strain in the films can be calculated. The calculated strain ϵ is plotted as a function of film thickness in Fig. 5. For Series B films, as the thickness increases, the sign of the strain ϵ along the film normal gradually changes from positive to negative. Thus the thinner films are subjected to a tensile strain, and films thicker than 130 nm are under a compressive strain. In the vicinity of 130 nm, then, the film is in a near stress-free condition. For Series A films, the strain decreases monotonically with increasing thickness, and in the vicinity of 200 nm the strain is almost equal to zero. It can be concluded from these results that the magnitude and sign of the strain in Co-Cr films are strongly influenced by the film thickness.

There are a number of possible explanations as to the origin of stress in the films. One is a perpendicular surface relaxation [17], [19] which results from a charge redistribution at the film surface due to the lowered symmetry of the surface electronic structure. In our case, the surface layer seems to experience a biaxial tensile strain when compared to the spatial distribution of the strain in the interior of the film. This observation is supported by the surface layer strain versus thickness curve plotted in Fig. 5. Here, the surface strain c_s was calculated by analysing the peak shift of the FCC (220) CoO phase. Auger depth profiling has proven [20]-[21] that at the outer surface (= 6A) of a Co-Cr film only the CoO and CoCr phases are present, while the inner oxide mainly consists of Cr_2O_3.

Another explanation for the observed film stress may be due to planar lattice misfits which may originate from a mismatch of the lattice spacing in the interfacial layer between the Co-Cr film and the Si substrate, as well as the Ge seedlayer if present. One last possible explanation may be that the planar film strain is caused by varying thermal expansion coefficients between the Co-Cr film and the substrate.

At present, there is no strong experimental evidence

TABLE III
THE DEPENDENCE OF THE PEAK SHIFT OF (0002) PLANES ON THE THICKNESS FOR SERIES A

No	A_1	A_2	A_3	A_4	A_5	A_6
Thickness (nm)	5	12	25	50	100	200
2θ (degree)	44.12°	44.35°	44.36°	44.45°	44.46°	44.49°

TABLE IV
THE DEPENDENCE OF THE PEAK SHIFT OF (0002) PLANES ON THE THICKNESS FOR SERIES B

No	B_1	B_2	B_3	B_4	B_5
Thickness (nm)	46	110	300	610	980
2θ (degree)	43.84°	44.49°	44.73°	44.84°	44.91°

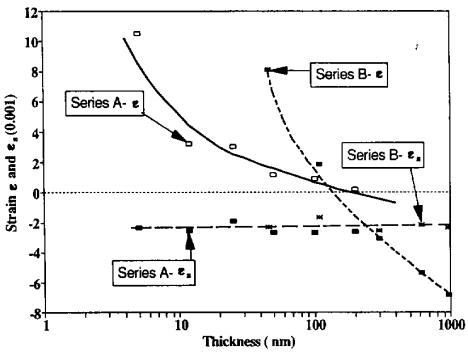

Fig. 5. The dependence of the strain of the whole film ϵ and the strain of surface layer ϵ_s on the thickness for Series A and B films.

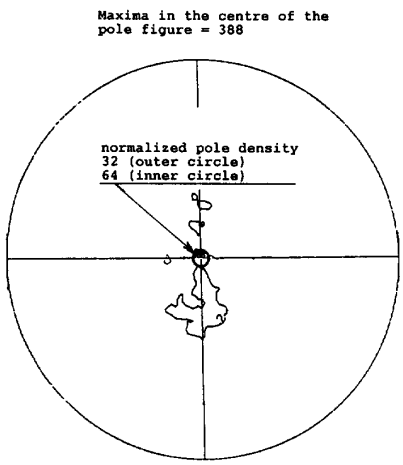

Fig. 6. The (0002) pole figure for specimen A_5 (100 nm).

pointing out which one, or combination of, these factors exert a dominant influence on the distribution pattern of the strain in the investigation $Co_{81}Cr_{19}$ films. However, the measured changes in the strain and texture for specimens having different thickness are closely related.

Typical results of the texture measurements are presented in the form of (0002) pole figures in Figs. 6 and 7 for specimen A_5 (100 nm) and A_2 (12 nm). As shown in

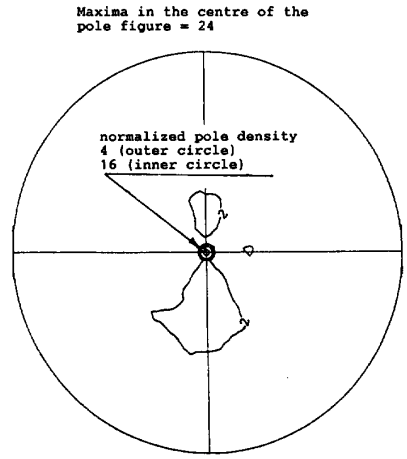

Fig. 7. The (0002) pole figure for specimen A_2 (12 nm).

Fig. 6, the 100 nm film exhibits a very strong texture with a maximum as high as 388 appearing at the centre of the (0002) pole figure. The pole figure consists of a series of very closely packed equal density curves in the centre which indicates a high degree of rotational symmetry. This demonstrates that the (0002) plane is aligned parallel to the specimen surface. Pole figures for the remainder of the Series A and B films have a very similar texture to that of the 100 nm thick film, the exception being that the strength of the texture varies.

To evaluate the magnitude of the orientation ratio and to determine the influence of texture development on the material magnetic properties, more precise distributions of the crystallographic orientation for all tested films were measured using the Siemens texture goniometer. Typical distribution curves of the (0002) poles in the vicinity of the film normal are shown in Figs. 8 and 9.

Using the measured pole density distribution and (1), the normalized orientation ratio $OR_c(\alpha)$ of the (0002) crystallographic planes can be calculated in random units. The angular dependence of the orientation ratio $OR_c(\alpha)$ for Series A and B films is presented in Figs. 10 and 11. It can be seen from Fig. 10 that, as the thickness increases

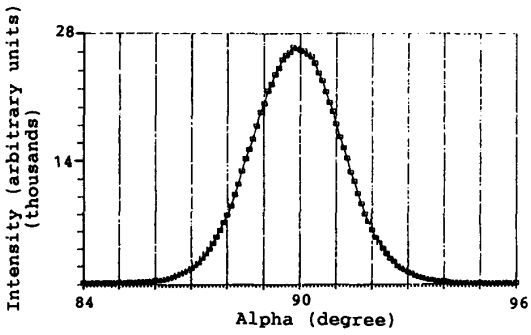

Fig. 8. (0002) pole density as a function of the specimen tilt angle α for specimen A_5 (100 nm).

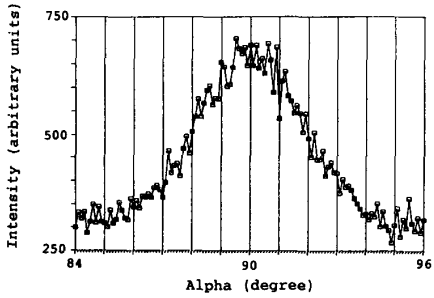

Fig. 9. (0002) pole density as a function of the specimen tilt angle α for specimen A_1 (5 nm).

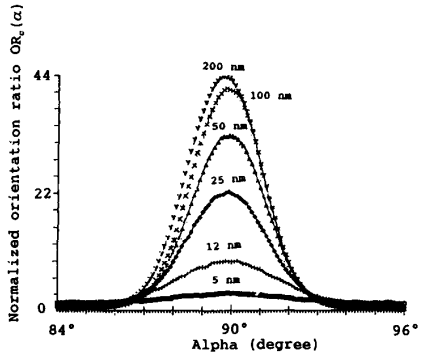

Fig. 10. The angular dependence of the orientation ratio $OR_c(\alpha)$ of the crystallite for Series A films having different thicknesses.

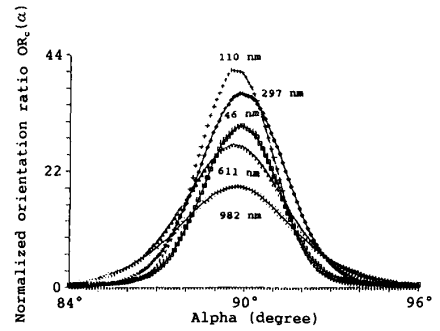

Fig. 11. The angular dependence of the orientation ratio $OR_c(\alpha)$ of the crystallite for Series B films having different thicknesses.

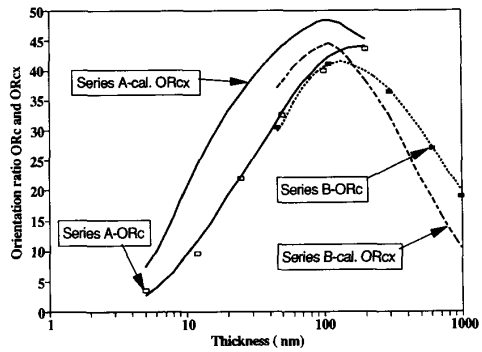

Fig. 12. The thickness dependence of the measured OR_c values and the calculated OR_{cx} values for Series A and B films.

from 5 to 200 nm for Series A films, the orientation ratio OR_c (maximum of $OR_c(\alpha)$) monotonically increases from 3.5 to 44. In the thinnest film of 5 nm the aspect ratio is close to 1, and grains are equiaxed. However, even in this film, the orientation ratio reaches 3.5, implying that (0002) texture is present, although the grains of the film do not exhibit a typical columnar shape.

Two important parameters are obtained from the angular dependence of the orientation ratio of the films: the peak value OR_c, reflecting the strength of (0002) texture and the $\Delta\alpha 50$ FWHM (full width-half maximum of the angular dependence of the OR_c curve), reflecting the dispersion of the C-axis. To obtain high quality perpendicular recording media, it is expected that a Co-Cr film should have the highest possible OR_c value and the lowest possible $\Delta\alpha 50$. The dependence of the peak orientation ratio OR_c on the thickness is plotted in Fig. 12 for both Series A and B films. For Series A films (5–200 nm), OR_c value increases constantly with increasing film thickness. For the Series B films, however, there is an optimum thickness where the maximum OR_c value appears near 130 nm. On the other hand, the dependence of $\Delta\alpha 50$ on the thickness in Fig. 13 shows that the optimum thickness, where the smallest $\Delta\alpha 50$ value is present, is at 50 nm and 80 nm for the Series A and B films. Thus the highest orientation ratio OR_c and the smallest $\Delta\alpha 50$ value do not appear at the same thickness. A comparison of the magnitude of changes in the orientation ratio OR_c and $\Delta\alpha 50$ shows that the relative changes of OR_c are much larger than those of $\Delta\alpha 50$. For example, for Series A films, when the film thickness changes from 5 to 200 nm, the relative change of OR_c is as high as 12.6, but the change rate of $\Delta\alpha 50$ is only 1.7. It will be demonstrated in our next two papers [10], [12] on this subject that the orientation ratio OR_m of the magnetization and the squareness ratio $R_s(M_r/M_s)$ for Co-Cr films are mainly determined by the orientation ratio OR_c of the crystallite, and only slightly influenced by $\Delta\alpha 50$. In view of this, it is recommended that

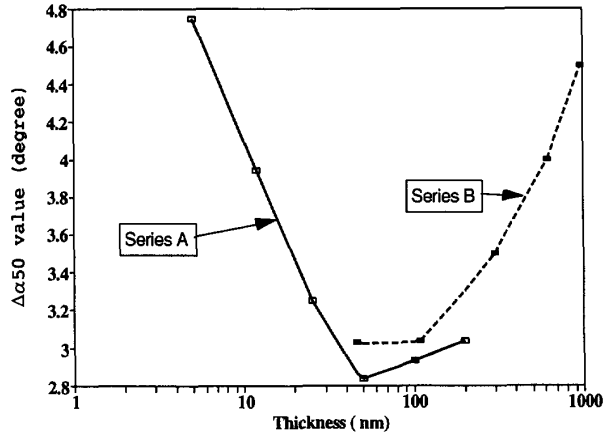

Fig. 13. The dependence of $\Delta\alpha 50$ on the thickness for Series A and B films.

OR_c is used to represent the degree of crystallographic orientation in Co–Cr films.

To explain why the orientation ratio of the crystallite decreases for films thicker than a critical value may involve the existence of stacking faults. These are considered to be related to internal stress. In general, it is believed [11], [17] that stacking faults may release some of the in-plane stress developed in films during grain growth. As well, based on observations made by other authors [6], [11], [16], columns themselves grow parallel to the film normal, but the C-axis deviates from the direction of the grain growth in varying degrees. This will cause the OR_c value to decrease in the thicker films.

The resulting orientation ratio OR_c and $\Delta\alpha 50$ value are determined by a balance between grain growth and stacking fault formation. Looking at the measured OR_c versus thickness curve for Series B films, if the film is thinner than the optimum value of 130 nm, the improvement of crystalline alignment is the dominant factor resulting in an increase of the OR_c value with increasing thickness. However, for a thickness greater than this optimum value, the number of stacking faults becomes dominant, and the dispersion of the hcp C-axes increases which decreases OR_c.

For an accurate analysis of experimental data, the influence of X-ray absorption (Mo–Kα radiation) on the pole density must be considered. This absorption is a function of the film thickness and the attenuation ratio η of the diffracted X-ray beam to the incident beam. This is given by [13]

$$\eta = \frac{dI_{DT(\text{at}x=T)}}{dI_{DO(\text{at}x=0)}} = \exp\left[-(2\mu T/\sin\theta)\right], \quad (2)$$

where dI_{DO} and dI_{DT} represent the intensities of the incident and diffracted beams. μ and T are the linear absorption coefficient and thickness of the thin film, and θ is the incident angle of the X-ray beam. Obviously, the X-ray intensity diffracted from the top layer of the films contributes much more to the pole density than a beam diffracted from the bottom layer. In order to separate the net local orientation ratio OR_{cx} of the crystallites for the x-th sublayer from the measured OR_c value, the film is assumed to be divided into x sublayers with different attenuation ratios η_x. The correlation between the normalized orientation ratio $OR_c(x)$ measured from the samples with changing thickness and the net local orientation ratio $OR_{cx}(x)$ corresponding to the x-th sublayer, corrected for the effect of X-ray absorption, can then be evaluated by the formulae [22]:

$$OR_{cx}(x) = OR_c(x) + \frac{1 - \exp(-\xi x)}{\xi}\frac{dOR_c(x)}{dx} \quad (3)$$

With

$$\xi = \frac{2\mu}{\cos\alpha \sin\theta} \quad (4)$$

where α and θ are the radial angles of the pole figure and the Bragg angle, and x represents the distance of the xth sublayer from the substrate along the film normal. The corrected local orientation ratio OR_{cx} of the crystallite as a function of thickness for the Series A and B films is shown in Fig. 12. It can be seen from this figure that both the Series A and B films exhibit almost the same optimum thicknesses near 110 nm.

Experimental data show that for Series A films, the OR_{cx} value is always larger than the measured OR_c value. In the case of Series B films, though the OR_{cx} value is larger than the OR_c value only for thicknesses less than 160 nm. This difference in the pattern of the change in the OR_{cx} and OR_c values for Series A and B films can be attributed to the effect of the different substrates. These results demonstrate that to obtain a high quality $Co_{81}Cr_{19}$ film with a high degree of crystallographic orientation, it is important to choose both the optimum film thickness and the proper substrate.

Finally, it is interesting to note that for Series B films both the highest orientation ratio OR_{cmax} and the lowest strain $\epsilon_{\min}$ are found for films whose thicknesses are about 130 nm. These conditions are very favourable for preparing high quality perpendicular recording media.

Conclusions

The following conclusions can be drawn from our experiments:

1) For the Series B $Co_{81}Cr_{19}$ films, the diameter of columnar grains increases with increasing thickness, with rapid increases taking place in films thinner than 200 nm. The aspect ratio vs. thickness curve exhibits a linear relation with film thicknesses up to 1000 nm. As the thickness increases from 40 to 1000 nm, the grain shapes gradually changes from equiaxial to conical shape.
2) In all tested films, the (0002) planes are well aligned with the film surface. The texture in the α-Co phase has a high degree of rotational symmetry around the film normal.

3) Experimental data shows that for Series B films, the orientation ratio of the (0002) planes as function of the film thickness has a single peak near 130 nm where the orientation ratio OR_c reaches its maximum value of 44. An analysis of the local orientation ratio OR_{cx} of the xth sublayers for Series A and B films shows the same optimum thickness (110 nm), where OR_{cx} values are as high as 48 and 45. In our case, it was found that the orientation ratio OR_c is the most sensitive measure of the degree of (0002) texture.
4) Both the orientation ratio OR_c and the strain ϵ of the whole film depend strongly on the film thickness. The surface strain, however, is almost independent of the thickness.
5) The aspect ratios for films thinner than 46 nm is about 1 with no typical columnar structure. However, for these films the number of textured (0002) planes is still about 3–4 times stronger than in a random specimen.

Acknowledgments

The authors acknowledge the financial support of the Natural Sciences and Engineering Research Council of Canada. We would like to thank Dr. W. Geerts and Dr. P. ten Berge, University of Twente, the Netherlands, for providing the samples and related experimental data of the magnetic properties. The authors are also obliged to Mr. S. Poplawski for doing the measurements on X-ray diffraction and texture. We are thankful to Mr. A. Morawiec for calculating OR_{cx} value.

References

[1] J. G. Zhu and H. N. Bertram, *IEEE Trans. Magn.*, vol. Mag-27, no. 4, pp. 3553-3562, 1991.
[2] S. Onodera, K. Ouchi, Y. Nakamura and S. Iwasaki, *J. of Magn. Society of Japan*, vol. 15, no. 2, pp. 163-166, 1991.
[3] C. H. L. Goodman, *Crystal Growth, Theory and Techniques*, 1974.
[4] K. Reichelt, *Vacuum*, vol. 38, pp. 1083-1098, 1988.
[5] P. ten Berge, C. Lodder, S. Porthum, and T. Popma, *J. Magn. Magn. Mater.*, vol. 113, pp. 36-46, 1992.
[6] H. Cura and A. Lenhart, *J. Magn. Magn. Mater.*, vol. 83, pp. 72, 1990.
[7] C. P. G. Schrauwen, J. P. C. Bernards, R. W. de Bie, G. J. P. van Engelen, H. H. Stel, V. Zieren, S. B. Luitjens, *IEEE Trans. Magn.*, vol. Mag-24, no. 2, pp. 1901, 1988.
[8] M. Mirzamaani, C. V. Jahnes and M. A. Russak, *IEEE Trans. Magn.*, vol. 28, no. 5, pp. 3090-3092, 1992.
[9] R. Hergt, H. Pfeiffer, and L. Fritzsch, *Phys. Sat. Sol.* (a) vol. 98, pp. 69-79, 1986.
[10] Li Cheng-Zhang, J. C. Lodder, and J. A. Szpunar, "The influence of the textural development on magnetic properties in $Co_{81}Cr_{19}$ films," *J. Magn. Magn. Mat.*, vol. 131, pp. 427-439, 1994.
[11] B. G. Demczyk, *J. Magn. Magn. Mater.*, vol. 102, pp. 238-246, 1991.
[12] Li Cheng-Zhang, J. C. Lodder, and J. A. Szpunar, "The effect of the composition and the substrate on the texture evolution and magnetic properties in Co-Cr films," *J. Magn. Magn. Mat.* (submitted).
[13] B. D. Cullity, "Elements of X-ray diffraction," 2nd Edition, 1978.
[14] R. S. Tebble and D. J. Craik, "Magnetic materials," pp. 68-73, 1969.
[15] J. C. Lodder, T. Wielinga, and J. Worst, *Thin Solid Films*, vol. 101, pp. 61, 1983.
[16] K. Hono, B. G. Demczyk, and D. E. Laughlin, *Appl. Phys. Lett.*, vol. 55, pp. 229, 1989.
[17] R. C. O'Handley and S-W. Sun, *J. Magn. Magn. Mater.*, vol. 104-107, pp. 117-1720, 1992.
[18] Ch. Morawe, A. Stierle, N. Metoki, K. Brohl, and H. Zabel, *J. Magn. Magn. Mater.*, vol. 102, pp. 223-232, 1991.
[19] B. G. Demczyk and J. O. Artman, *J. Phys. D: Appl. Phys.*, vol. 24, pp. 1627-1632, 1991.
[20] W. J. M. A. Geerts, J. C. Lodder, and Th. J. A. Popma, *J. Magn. Magn. Mater.*, vol. 104-107, pp. 971-972, 1992.
[21] T. Masuda, W. J. M. A. Geerts, and J. C. Lodder, *J. Magn. Magn. Mater.*, vol. 95, pp. 123-132, 1991.
[22] A. Morawiec, "Pole figures of through-thickness inhomogeneous samples," internal report, McGill University, Montreal, Canada, 1992.

Li Cheng-Zhang, biography not available at the time of publication.

J. C. Lodder, biography not available at the time of publication.

J. A. Szpunar, biography not available at the time of publication.